

Transmission properties and effective electromagnetic parameters of double negative metamaterials

Peter Markoš^{1,2,3} and C. M. Soukoulis^{1,3}

¹ Ames Laboratory and Dept. of Physics and Astronomy, Iowa State University, Ames, Iowa, 50011

² Dept. of Complex Physical Systems, Institute of Physics, Slovak Academy of Sciences, 845 11 Bratislava, Slovakia

³ Research Center of Crete, POB 1572, 71110 Heraklion, Crete, Greece

markos@savba.sk, soukoulis@ameslab.gov

Abstract: We analyze the transmission properties of double negative metamaterials (DNM). Numerical simulations, based on the transfer matrix algorithm, show that some portion of the electromagnetic wave changes its polarization inside the DNM structure. As the transmission properties depend strongly on the polarization, this complicates the interpretation of experimental and numerical data, both inside and outside of the pass band. From the transmission data, the effective permittivity, permeability and refractive index are calculated. In the pass band, we found that the real part of permeability and both the real and the imaginary part of the permittivity are negative. Transmission data for some new structures are also shown. Of particular interest is the structure with cut wires, which possesses two double negative pass bands.

© 2003 Optical Society of America

OCIS codes: 000.2690, General physics; 000.4430 Numerical approximation and analysis

References and links

1. J.B. Pendry, A.J. Holden, W.J. Stewart and I. Youngs, "Extremely Low Frequency Plasmons in Metallic Mesostructures," *Phys. Rev. Lett.* **76**, 4773 (1996)
2. J.B. Pendry, A.J. Holden, D.J. Robbins and W.J. Stewart, (1999) "Magnetism from conductors and enhanced nonlinear phenomena," *IEEE Trans. on Microwave Theory and Techn.* **47**, 2075 (1999)
3. D.R. Smith, W.J. Padilla, D.C. Vier, S.C. Nemat-Nasser, and S. Schultz "A Composite medium with simultaneously negative permeability and permittivity," *Phys. Rev. Lett.* **84**, 4184 (2000)
4. D.R. Smith and N. Kroll, "Negative Refractive Index in Left-Handed Materials," *Phys. Rev. Lett.* **85**, 2933 (2000)
5. R.A. Shelby, D.R. Smith, S.C. Nemat-Nasser, and S. Schultz, "Microwave transmission through a two-dimensional, isotropic, left-handed meta material," *Appl. Phys. Lett.* **78**, 489 (2001)
6. P. Markoš and C.M. Soukoulis, "Transmission Studies of the Left-handed Materials," *Phys. Rev. B* **65** 033401 (2002)
7. P. Markoš and C.M. Soukoulis, "Numerical Studies of Left-handed materials and Arrays of Split Ring Resonators" *Phys. Rev. E* **65**, 036622 (2002)
8. P. Markoš, I. Rousochatzakis, and C.M. Soukoulis, "Transmission Losses in Left-handed Materials," *Phys. Rev. E* **66**, 045601 (2002)
9. C. D. Moss, T. M. Grzegorzcyk, Y. Zhang, and J. A. Kong, "Numerical Studies of Left-handed Metamaterials," *Progress In Electromagnetics Research, PIER* **35**, 315 (2002)
10. V.G. Veselago, "The electrodynamics of substances with simultaneously negative values of permittivity and permeability," *Sov. Phys. Usp.* **10**, 509 (1968)

11. M.M. Sigalas, C.Y. Chan, K.M. Ho, and C.M. Soukoulis, "Metallic photonic band-gap materials," *Phys. Rev. B* **52**, 11744 (1999)
12. R.A. Shelby, D.R. Smith, and S. Schultz, "Experimental verification of a negative index of refraction," *Science* **292**, 77 (2001)
13. C. G. Parazzoli, R. B. Gregor, K. Li, B. E. C. Koltenbah, and M. Tanielian, "Experimental Verification and Simulation of Negative Index of Refraction Using Snell's Law," *Phys. Rev. Lett.* **90** 107401 (2003)
14. D.R. Smith, S. Shultz, P. Markoš, and C.M. Soukoulis, "Determination of Effective Permittivity and Permeability of Metamaterials from Reflection and Transmission Coefficient," *Phys. Rev. B* **65** 195104 (2002)
15. D. R. Smith and D. Schurig, "Electromagnetic Wave propagation in Media with Indefinite Permittivity and Permeability Tensors," *Phys. Rev. Lett.* **90** 077405 (2003)
16. S. O'Brien, and J.B. Pendry, "Photonic band gap effects and magnetic activity of dielectric composites," *J. Phys.: Condens. Matter* **14** 4035 (2002)
17. J.B. Pendry and A. MacKinnon, *Phys. Rev. Lett.* **69** 2772 (1992)
J.B. Pendry, "Photonic band gap structures," *J. Mod. Opt.* **41** (1994) 209
J.B. Pendry and P.M. Bell 1996, "Transfer matrix techniques for electromagnetic waves," in *Photonic Band Gap Materials* vol. **315** of NATO ASI Ser. E: Applied Sciences (1996), ed. by C.M. Soukoulis (Plenum, NY) p. 203
18. *Photonic Band Gap Materials*, ed. by C.M. Soukoulis (Kluwer, Dordrecht, 1996); *Photonic Crystals and Light Localization in the 21st Century*, ed. by C.M. Soukoulis (Kluwer, Dordrecht, 2001)
19. P. Markoš and C. M. Soukoulis, "Absorption losses in periodic arrays of thin metallic wires", *e-print cond-mat/0212343* to appear in *Opt. Lett.* (2003)
20. L.D. Landau, E.M. Lifshitz, and L.P. Pitaevskiĭ, "Electrodynamics of Continuous Media," Pergamon Press 1984
21. E.V. Ponizovskaya, M. Nieto-Vesperinas, and N. Garcia, "Losses for microwave transmission metamaterials for producing left-handed materials: The strip wires," *Appl. Phys. Lett.* **81**, 4470 (2002)
22. J.D. Jackson, "Classical Electrodynamics," (3rd edition), J.Wiley and Sons, 1999, p. 312
23. M. Bayindir, K. Aydin, E. Ozbay, P. Markoš, and C.M. Soukoulis, "Transmission Properties of Composite Metamaterials in Free Space," *Appl. Phys. Lett.* **81**, 120 (2002)
24. E. Ozbay, K. Aydin, E. Cubukcu, and M. Bayindir, "Transmission and reflection properties of composite double negative metamaterials in free-space," to be published (2003)
25. P. Markoš, D.R. Smith, and C.M. Soukoulis, unpublished.
26. R. Ruppin, "Electromagnetic energy density in a dispersive and absorptive material," *Phys. Lett. A* **299** 309 (2002)

1. Introduction

Theoretical work of Pendry *et al.* [1, 2] inspired the fabrication [3], theoretical [4], experimental [5] and numerical [6, 7, 8, 9] studies of double negative metamaterials (DNM). "Double negative" means that these structures have, in a given frequency interval, both the effective permittivity ϵ_{eff} and permeability μ_{eff} *negative*. They are also called "Left-handed materials" (LHM) after Veselago [10], who discussed some unusual physical properties of the DNM over 30 years ago.

The structural design of DNM was described in many previous papers. Here we only show in Fig. 1 the typical structure of the unit cell. Generally speaking, DNM are created by a combination of a periodic array of thin metallic wires and an array of split ring resonators (SRR). An array of thin metallic wires creates a negative- ϵ medium with the effective permittivity ϵ_{eff} given by the formula [1, 11]

$$\epsilon_{\text{eff}} = 1 - \frac{f_e^2}{f^2 + i\gamma_e f} \quad (1)$$

An array of split ring resonators (SRR), on the other hand, is responsible for the resonant form of the effective magnetic permeability. The theoretical formula [2] is given by

$$\mu_{\text{eff}} = 1 - \frac{F f^2}{f^2 - f_m^2 + i\gamma_m f}, \quad (2)$$

In Eqs. (1) and (2), f_e is the electronic plasma frequency, f_m is the magnetic resonance frequency, γ_e (γ_m) represent the losses of the system, and F is a filling factor of the SRR.

Maxwell's equations demonstrate that electromagnetic (EM) wave can easily propagate in a material with both ϵ and μ negative [10]. This seems to be confirmed by experiments [3] and by numerical simulations [6]. An increase of the transmission by many orders of magnitude inside the resonance frequency interval in which ϵ and μ are expected to be negative, is consistent with the theoretical prediction. The experimental data for the transmission only, however, can not prove that ϵ and μ are indeed negative. The experimental proof of the negative n was done by measuring the *negative* Snell's law [12, 13]. Negativeness of the effective index of refraction, ϵ_{eff} and μ_{eff} has been proved by the analysis of numerical data, for the transmission and reflection (magnitude as well as phase) obtained by the transfer matrix method (TMM) [14].

In practice, however, the problem of the estimation of the effective parameters is more complicated. Firstly, the structures investigated at present (Fig. 1) are strongly anisotropic. Both permittivity and permeability are tensors with negative components $\mu_{zz} < 0$ and $\epsilon_{xx}, \epsilon_{yy} < 0$ only [15]. One observes the "left-handed" properties only when EM wave propagates along the z axis. No wave propagation is possible along the x or the y axis since the product $\epsilon\mu$ is negative for this direction. This might be overcome using more sophisticated structures. For instance, structures analyzed in Refs. [5, 12] exhibit left-handed properties for any wave propagation perpendicular to wires and are effectively two-dimensional. We are not aware of any three-dimensional structures. Besides the anisotropy, the permittivity and permeability tensors are not diagonal. Small off-diagonal elements are responsible for the change of the polarization inside the sample. This plays an important role in the interpretation of the experimental data. We note also that both ϵ and μ are complex.

In this paper, we use the transfer matrix method for the analysis of the transmission of EM waves through the DNM. Transfer matrix is introduced briefly in Section 2. We discuss in Section 3 the transmission data for both polarizations of the EM wave. The fact that some portion of the EM wave changes its polarization inside the DNM structure might complicate the interpretation of experiments, as well as the analysis of the effective parameters ϵ and μ . In Section 4 we use the data for transmission and reflection to calculate the effective parameters of various metamaterials. We show that in the resonance frequency interval DNM indeed possesses negative effective permittivity, permeability and negative refractive index. More detailed analysis shows that not only the real part of permittivity ϵ'_{eff} , but also the *imaginary* part ϵ''_{eff} is *negative*. The same was observed in other structures [16]. This is a surprising result because the imaginary parts of permittivity and permeability are associated with transmission losses. There is a common belief that they should be positive in passive materials. We discuss this result in Section 5. In Section 6 we propose some new designs of DNM and calculate their transmission properties. Of particular interest is the structure with cut wires which possesses more than one DNM pass band.

2. Transfer matrix method (TMM)

For the numerical analysis of the DNM, we apply our version [6, 7] of the transfer matrix technique, inspired by the original algorithm developed by Pendry and co-workers [17]. Due to the periodic structure of the DNM, we only concentrate on one unit cell as is shown in Fig. 1, and use periodic boundary conditions in the lateral directions. For details of the simulation and the numerical algorithm, see Ref. [7].

The main approximation, used in the TMM, is the discretization of Maxwell's equations. The TMM is supposed to be more accurate for more detailed discretization, which,

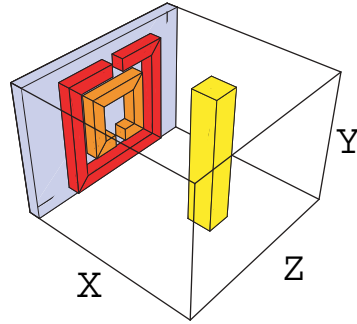


Fig. 1. Typical DNM structure consists of periodic array of split-ring resonators (SRRs), combined with periodic arrangement of thin metallic wires. The structure is symmetric in all lateral directions. Only one unit cell is shown. This structure possesses negative permittivity and permittivity only for a wave, propagating in the z direction and polarized with $\vec{E}||y$ [3].

however, increases the size of the transfer matrix, and thus the numerical simulations require longer time. Fortunately, various applications of the TMM in the analysis of the transmission of EM waves in photonic band gap structures (for details, see Ref. 15) confirmed, that the results of the TMM simulations agree satisfactorily with the experimental data. However, DNM contain metallic components, which possess very large and complex values of the metallic permittivity $\epsilon_m = \epsilon'_m + i \epsilon''_m$. In our simulations, ϵ''_m takes values as large as 10^6 . In such strongly inhomogeneous structures there is a danger that the discretization of Maxwell's equation might not be accurate enough. Therefore, in order to check the ability of the transfer matrix to give us the proper electromagnetic parameters of the LH structure, we analyzed the simpler system, namely the periodic array of thin metallic wires. Thanks to the translational invariance of this system along the wire axis, the system is effectively two-dimensional. This enabled us to use various

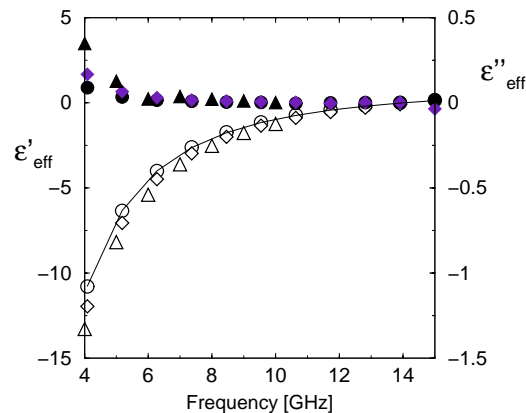


Fig. 2. Effective permittivity for an array of thin square metallic wires of the size of $200 \times 200 \mu\text{m}$. Closed symbols shows the imaginary part ϵ''_{eff} , open symbols are for the real part ϵ'_{eff} . The period of the square lattice is $a = 5 \text{ mm}$. Three different discretizations of the unit cell were used, in which the wire is represented by 1×1 (circles), 2×2 (diamonds) and 4×4 (triangles) mesh points. Solid line is a fit of the data to the analytical formula (1). Data confirm the stability of the transfer matrix simulations, at least in the frequency interval $f > 6 \text{ GHz}$. Permittivity of the metal is $\epsilon_m = -2000 + 10^6 i$. More detailed numerical analysis of the effective permittivity of array of metallic wires was performed in Ref. [19].

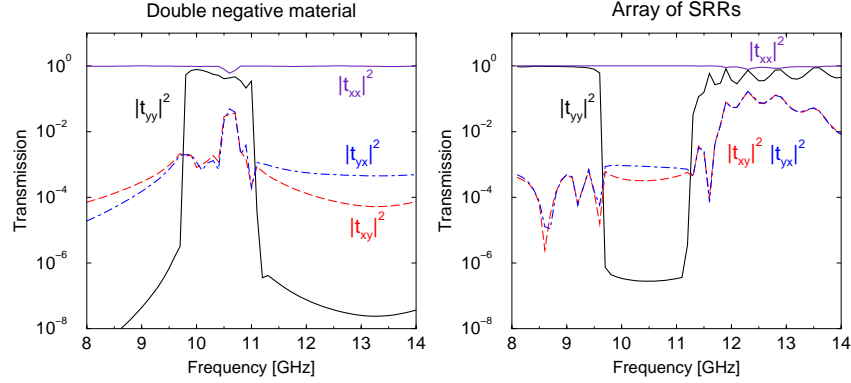


Fig. 3. Left: Transmission $|t_{yy}|^2$, $|t_{xx}|^2$, $|t_{xy}|^2$, and $|t_{yx}|^2$ for a DNM structure shown in Fig. 1. Periodic boundary conditions are considered in the x and y directions. The length of the system is 20 unit cells along the z direction. The transmission t_{yy} clearly determines the resonance interval (9.8-11 GHz), where we expect the permittivity and permeability to be both negative. Note that the “off-diagonal” transmissions t_{xy} and t_{yx} are much higher than t_{yy} outside the resonance interval. Right: the same for an array of SRR only.

discretizations of the unit cell. As it is shown in Fig. 2, the obtained effective permittivity is almost independent of the discretization procedure.

In the analysis of the DNM, we are able to use discretization up to $N = 10^3$ mesh points per unit cell. More detailed discretization will require too long CPU time. As we only use a homogeneous discretization, we are restricted in the sizes of the DNM structures. All the length scales of the DNM are namely given as multiples of the minimum mesh length which is typically 0.15-0.33 mm.

3. Transmission data

For the DNM shown in Fig. 1, the left-handedness is observable only when an EM wave propagates along the z direction (Fig. 1). The transfer matrix can obtain not only the transmission for both the $\vec{E}||y$ polarization (t_{yy}) and the $\vec{E}||x$ polarization (t_{xx}), but also the transmission t_{xy} and t_{yx} . The last two transmissions give the change of the polarization of the EM wave inside the structure.

In Fig. 3 we show all the transmissions $|t|^2$ for the DNM as shown in Fig 1 and for an array of SRR. Note that the “off-diagonal” transmissions $|t_{xy}|^2$ and $|t_{yx}|^2$ are relatively large also in the band pass of DNM. This means that in the DNM structure, there always exists a possibility for the transmission from one polarization wave into the other one. This effect plays an important role outside the band pass. In Fig. 4 we show the transmission for the DNM structure for the frequency $f = 9.7$ GHz, which is slightly below the lower pass band edge. We see that for a system length shorter than 10 unit cells, the transmission quickly oscillates and decreases exponentially. This indicates that both $|n'_{\text{eff}}|$ and $|n''_{\text{eff}}|$ are large. After passing 10 unit cells, however, the transmission stops to decrease and its length dependence is determined by the index of refraction in vacuum.

The origin of this effect is easy to understand. The total transmission t_{yy} consists not only from the “unperturbed” contribution $t_{yy}^{(0)}$, but also from additional terms, which describe the conversion of the y -polarized wave into x -polarized and back to y -polarized:

$$t_{yy}(0, L) = t_{yy}^{(0)}(0, L) + t_{yy}^{(1)} \quad (3)$$

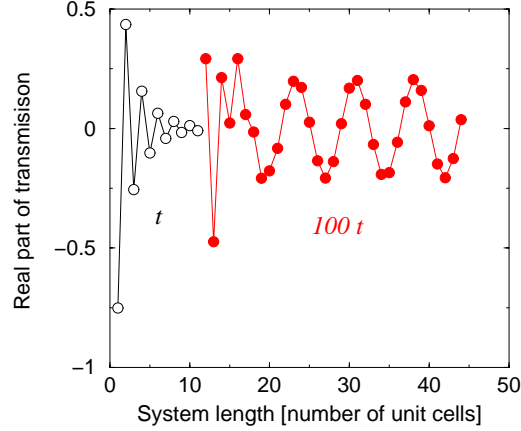


Fig. 4. Real part of the transmission t_{yy} for a system on the left side ($f = 9.7$ GHz) of the DNM pass band. Open symbols show the transmission t_{yy} , closed symbols show the transmission multiplied by factor of 100 for a longer system length. Data show that the amplitude of the transmission does not decrease after passing more than 12 unit lengths. The spatial dependence of t_{yy} is given by $n = 1$, in agreement with Eq. 3

where

$$t_{yy}^{(1)} = \sum_{z, z'} t_{yx}(0, z) t_{xx}(z, z') t_{xy}(z' L) + \dots \quad (4)$$

In Eq. (3) the transmission $t_{yy}^{(0)}(0, L)$ decreases exponentially with the system length L , while the second term $t_{yy}^{(1)}$, which represents the conversion of the y -polarized wave into x -polarized wave and back, remains system-length independent, because $t_{xx}(z, z') \sim 1$ for any distance $|z - z'|$. For system length larger than certain “critical length”, one observes only the term $t_{yy}^{(1)}$. For example in Fig. 4, the “critical length” is 10 unit cells. For other frequencies, for which n''_{eff} is larger, the “critical length” decreases to 1-2 unit cells. Therefore, in the experiment, one observes only the transmission given by the second term of Eq. (3).

It is worth mentioning that $t_{yy}^{(1)}$ might play an important role also inside the band pass, where the first term $t_{yy}^{(0)}$ decreases only slowly with the system length. The total transmission, measured *outside* the sample always contains a small portion of the $\vec{E}||y$ wave, which *inside* the structure behaves as $\vec{E}||x$ and knows nothing about the negativity of effective parameters. In our numerical simulations, the amplitude of this “false wave” is rather small. In Fig 3, the transmission $|t_{yx}|^2$ is of the order of 10^{-3} (with sharp maximum $|t_{xy}|^2 \approx 0.036$ for $f = 10.7$ GHz). This means that $|t_{yy}^{(1)}|$ is 4-5 orders of magnitude smaller than the total transmission. However, contrary to the transmission $|t_{yy}^{(0)}|$, which always decreases as a function of the system length, $|t_{yy}^{(1)}|$ is system-length independent, so that it might be possible to observe it experimentally when large samples are measured. Note also that we can not exclude that t_{xy} is much larger for some other DNM pass band.

4. Effective parameters of DNM

The transmission and reflection of EM waves through a homogeneous slab of width L are given, in terms of the index of refraction n and impedance z of the slab, by the

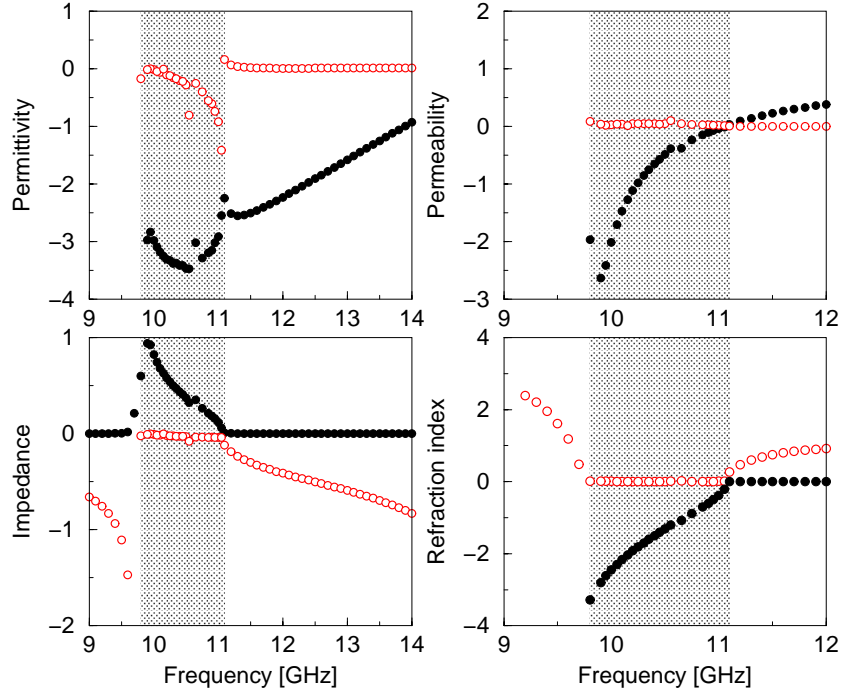


Fig. 5. Effective permittivity, permeability, impedance and index of refraction for the DNM structure shown in the Fig.1. Solid (open) circles denote real (imaginary) part, respectively. Dashed area shows the left-handed frequency band. Note that not only ϵ'_{eff} and μ'_{eff} but also imaginary part of the permittivity, ϵ''_{eff} is negative. Outside the pass band and for frequencies $f < 9.8$ GHz, we did not succeed to find the real part of the refractive index. The spatial oscillations of the transmission are very fast indicating that $|n'_{\text{eff}}| > 4$. Then, the wavelength of the EM wave becomes comparable with the size of the unit cell and the proper value of n'_{eff} is not accessible.

textbook formulas

$$t^{-1} = \left[\cos(nkL) - \frac{i}{2} \left(z + \frac{1}{z} \right) \sin(nkL) \right], \quad (5)$$

and

$$\frac{r}{t} = -\frac{i}{2} \left(z - \frac{1}{z} \right) \sin(nkL), \quad (6)$$

respectively. Here, k is the wave vector in vacuum of the normally incident EM wave. Our aim is to invert Eqs. (5) and (6), i.e., to express n and z as a function of t and r . Once n and z are obtained, permittivity and permeability can be easily calculated from the relations

$$\epsilon = n/z \quad \text{and} \quad \mu = nz. \quad (7)$$

We invert the expressions for the transmission and the reflection and obtain that

$$z = \pm \sqrt{\frac{(1+r)^2 - t^2}{(1-r)^2 - t^2}} \quad (8)$$

with sign on the r.h.s determined by the requirement

$$z' > 0, \quad (9)$$

and

$$\cos(nkL) = X = \frac{1}{2t} (1 - r^2 + t^2). \quad (10)$$

Equation (10) gives

$$e^{-n''kL} [\cos(n'kL) + i \sin(n'kL)] = Y = X \pm \sqrt{1 - X^2}. \quad (11)$$

The sign in the r.h.s of Eq. (11) is determined by the requirement

$$n'' > 0, \quad (12)$$

which assures that the amplitude of the EM wave decreases inside the structure ($|Y| < 1$). This determines unambiguously both real and imaginary part of the refractive index.

For a given system length L , relation (11) enables us to find unambiguously both the real and the imaginary part of the index of refraction. We collect the data for various system lengths L , and calculate n' and n'' from the linear fits of $n''kL$ and $n'kL$ versus the system length L .

The effective parameters of the DNM, obtained by the present method, are shown in Fig. 5. The obtained results unambiguously confirm that the real part of the refractive index is negative in the resonance frequency interval (pass band). Also ϵ'_{eff} and μ'_{eff} have been found to be negative.

There are two main constrains of the present method:

(1) it works only when

$$|t_{xy}| \ll |t_{yy}|. \quad (13)$$

For the structure shown in Fig. 1, this condition is fulfilled only inside the pass band (Fig. 3). For smaller frequencies, $|t_{xy}|$ is much larger than $|t_{yy}|$ already for a system length of 2-3 unit cells. As we will discuss later, for more complicated structures the condition (13) is not satisfied even in the pass band. Then, the method used by Smith *et al.* must be applied [14]. For the determination of the effective parameters, they used only the transmission and reflection data for short system lengths. The ambiguity of the solution is avoided by the requirement that all the parameters must be continuous functions of the frequency.

(2) The analysis of the transmission data of the DNM, assumed that the wavelength λ of the EM wave is much larger than the spatial period of DNM. The wavelength λ is of order of cm in the GHz region. The typical size of the inhomogeneity, measured by the size of the unit cell shown in Fig. 1 is 5-10 times smaller than the wave length. In spite of the small value of the ratio wavelength/(size of the unit cell) we believe that our data are relevant. One can obtain much larger ratio wavelength/(size of the unit cell) in the frequency interval where n' is negative, but $|n'| < 1$. We can also improve the ratio wavelength/(size of the unit cell), by filling the structure with a dielectric with a high permittivity ϵ_d . This reduces the resonance frequency of the SRR by factor $\epsilon_d^{-1/2}$. We performed numerical simulations for $\epsilon_d = 10$ (data not shown here) and observed the same qualitative behavior of the effective parameters as in this paper.

However, close to the left boundary of the pass band, $|n'_{\text{eff}}|$ becomes so large that λ is comparable with the size of the unit cell. In this frequency region Eqs. (5) and (6) are not sufficient to estimate n .

In spite of the above mentioned constrains, we conclude that the frequency dependence of the magnetic permeability μ_{eff} follows the analytical formula (2). The same was observed in Ref. [14] The frequency dependence of the effective permittivity ϵ_{eff} is more complicated. It is evident that it can not be described by simple relation (1). We found the non-monotonic frequency-dependence of ϵ'_{eff} , again in agreement with previous results [14]. The real part of ϵ_{eff} exhibits peaks at frequencies where n'_{eff} or μ'_{eff} change their sign.

5. Negative ϵ''_{eff} materials?

As is shown in Fig. 5, the imaginary part of the effective permittivity is negative in the left handed band. Data shown in Fig. 5 even indicate that both ϵ'_{eff} and ϵ''_{eff} exhibits resonant behavior in the neighborhood of the frequency f' where $\mu'_{\text{eff}}(f') = 0$. This is easy to understand mathematically. Relation $n^2 = \epsilon\mu$ gives for the real and the imaginary part of the refractive index

$$n'^2 - n''^2 = \epsilon'\mu' - \epsilon''\mu'' \quad (14)$$

and

$$2n'n'' = \epsilon'\mu'' + \epsilon''\mu' \quad (15)$$

From Eq. (15) $\epsilon'' = (2n'n'' - \epsilon'\mu'')/\mu'$ indeed has a poles at frequency f' and changes its sign from negative (for $f < f'$) to positive (for $f > f'$).

We observed numerically that $|n'| \gg n''$ for frequencies $f \leq f'$. Then the r.h.s. of Eq. (14) must be positive in the limit $f \rightarrow f'$. As the product $\epsilon'\mu' \rightarrow 0$ for $f \rightarrow f'$, Eq. (14) implies that the product $\epsilon''\mu''$ is *negative* for $f \leq f'$. Hence the small value of n''_{eff} implies not only very good transmission properties of DNM, but also negativeness of ϵ'' .

It is natural to test whether the negative sign of ϵ''_{eff} is not a result of oversimplified model Eqs. (5) and (6). The generalization of the relations Eqs. (5) and (6) to anisotropic systems would be desired, which calculate tensors of the permittivity and permeability from all transmission data t_{yy} , t_{xx} , t_{xy} and t_{yx} . However, the transmission t_{xy} is small: $|t_{xy}|^2 < 10^{-3}$ for $f \leq 11$ GHz, while $|t_{yy}^{(0)}| \sim 5 - 8 \times 10^{-2}$ for the system lengths 200-300 unit cells. Therefore the correction to transmission, given by Eq. (4), is $|t_{yy}^{(1)}| \sim 10^{-3} \ll |t^{(0)}|$. We assume therefore that the “off diagonal” transmissions would only smooth the “resonance” behavior of ϵ'' . The qualitative frequency dependence would be unchanged. We note also that the negative ϵ''_{eff} was observed in the system of dielectric wires, [16] in which, because of the the translational symmetry of the system along the wires the permittivity and permeability tensors are *diagonal* so that $t_{yy}^{(1)} \equiv 0$.

It is highly desired to support the negativeness of the ϵ''_{eff} by a more detailed theoretical analysis. To the best of our knowledge, there is no theoretical work which determine the energy and the losses of the EM wave propagated in the medium with arbitrary values of (complex) ϵ and μ . Nevertheless, we note that the negative sign of the ϵ'' is not in contradiction with any physical law. In particular, the transmission losses, which are usually expressed in terms of ϵ'' and μ'' [20] could be re-written, at least in the special case of the normally incident plane wave, in terms of n'' and z' as

$$Q = \frac{1}{2\pi} \int d\omega \omega |H|^2 \times 2n''(\omega)z'(\omega) \quad (16)$$

which is always positive, independently on the sign of ϵ'' and μ'' because n'' and z' are positive (see Eqs. (12) and (9)). We did not find any general analysis of the transmission losses in systems with arbitrary sign and values of the (complex) permittivity and permeability.

We believe that our results are also in agreement with Kramers-Kronig relations [20]. However, a direct numerical test of this is difficult since we can not find the permittivity and permeability for all frequencies. Not only in the limit $f \rightarrow \infty$, but also at the left boundary of the pass band, the permittivity and permeability is not achievable by present methods.

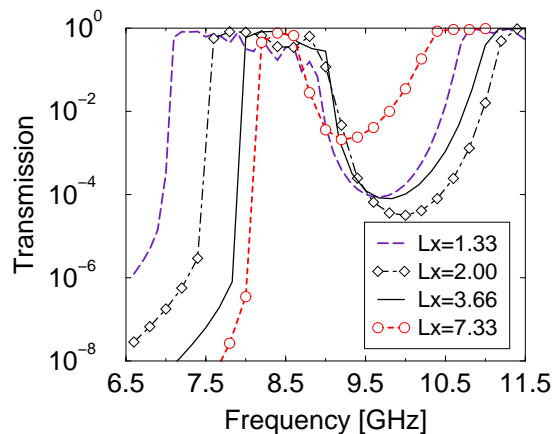


Fig. 6. Dependence of the transmission peak on the shape of the unit cell. In this simulations, the wire is deposited on the opposite side of the dielectric board. The width of the transmission band increases as the width of the unit cell decreases. Calculation of the effective refraction index (data not shown) confirmed that the band is left-handed with $n_{\text{eff}} < 0$.

6. Other one-dimensional DNM structures

The transmission properties of the DNM depend strongly on the structure of the unit cell. Even for the standard unit cell, shown in Fig. 1, the transmission depends on the structural parameters of the SRR, on the orientation of gaps of SRR, on the mutual position of wire and SRR, on the value of dielectric constant of the medium in which the metallic components resides. Qualitative analysis of these dependences is possible by the use of the TMM and was given in Ref. [7].

As an example of how strong the transmission depends on the shape of the unit cell, we show in Fig. 6 the transmission peaks for various widths of the unit cell. One sees that the width of the transmission band increases as the mutual distance of the SRR (measured by the size of the unit cell along the x direction) decreases

Of particular interest is the role of the wire in the DNM structure. It is important to know how the size and thickness of the metallic wire influences the transmission properties. We analyzed therefore also the effective parameters of the periodic array of thin metallic wires [19]. Results already presented in Fig. 2 confirm that the imaginary part of the effective permittivity is very small. The damping parameter γ , obtained from the fit of the numerical data to Eq. (1) is only 0.003 GHz. For thinner wires, γ increases, but still is relatively low. The losses are also small for the wires used in the experiments on the negative Snell's law [5, 12]. Even for wires of size $30 \times 30 \mu\text{m}$ the transmission losses are small. Contrary to others [21], we concluded [19], that the low transmission, observed in the pioneering experiments [3, 5] was not due to the absorption of the electromagnetic wave in the material, but rather due to the scattering losses, or, maybe, due to the losses in the dielectric material on which SRR were deposited [8].

Very promising results were recently obtained in experiments in which the wire was deposited on the dielectric board on the same side with the SRR [23]. Another structure, which used cut wires instead of continuous ones, was investigated experimentally in Ref. [24] Inspired by these results, we simulated such structures with either continuous or cut wires. The two typical structures and the obtained transmission data are shown in Figs. 7 and 8.

In Fig. 7 we present the transmission *versus* frequency for a DNM used in the experiment of Ref. [23]. Notice that the transmission peak is broader than that presented

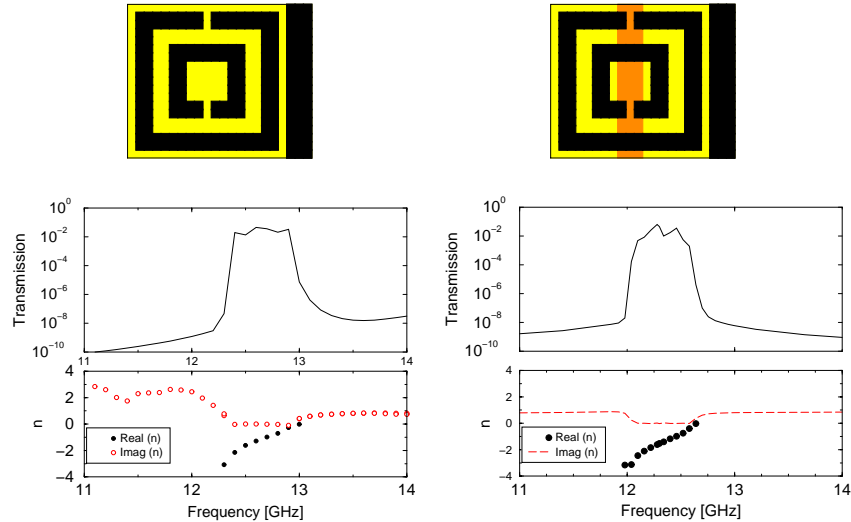


Fig. 7. Left: Transmission and the refraction index (bottom) for a one-dimensional DNM in which the wire is positioned along the SRR as shown in the top figure. The size of the unit cell is $1.764 \times 3.35 \times 3.84$ mm. The size of the SRR is 3×3 mm. Azimuthal gap $g = 0.176$ mm, radial gaps and width of rings is 0.35 mm. The wire width are 0.53 mm. The permittivity of the metallic components $\epsilon_m = -2000 + 10^6 i$. Data for the refraction index confirm the left-handedness of the pass band. Right panel shows the same structure with one additional wire located on the opposite side of the dielectric board.

in Ref. [23], because the distance between the SRR is much smaller (1.764 mm) than in the previous one (5 mm). This agrees with our results mentioned above (Fig. 6). Notice also that indeed the real part of refractive index is negative, while the imaginary part is very small inside the pass band. The right panel of Fig. 7 shows the same structure to which one additional wire on the opposite site of the dielectric board is added. Transmission data confirm that this wire does not play any significant role, only decreases the position of the DNM band pass by approximately 0.3 GHz.

In Fig. 8 we present results for the structure which has also the metallic wires in the same side of the dielectric board as the SRR. However, in this case the metallic wires are cut. This makes an important difference. The transmission coefficient *versus* frequency for a lattice of cut wires is shown by a dashed line on the top panel of Fig. 8. The transmission is close to one for frequencies up to 10 GHz and drops to very small values for higher frequencies. So that the behavior of the cut wires is completely different from that of continuous wires. While the continuous wires behave as high pass filters, the cut wires behave as photonic crystals [25]. As can be seen from the bottom panel of Fig. 8, the first transmission peak of the DNM gives a positive index of refraction, and the two higher peaks give negative index of refraction.

The existence of two double negative pass bands is surprising, since this requires two resonance frequencies of SRR. To the best of our knowledge, this is the first time that two double negative pas band were observed in the same structure. When compared with the results for continuous wires, we see that the position of DNM pass band increases considerably: the first band appears for frequencies 16.5-18 GHz, the second band for frequencies 20.5-23 GHz. While the width of bands is due to small distance between SRR (see also Fig. 6). The increase of the resonance frequency is probably due to the cut of the wires.

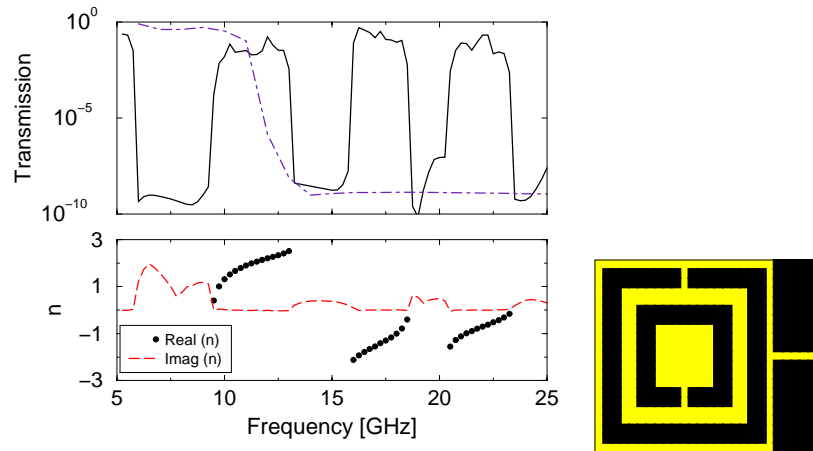


Fig. 8. Transmission (top) and the refractive index (bottom) for a one-dimensional DNM with cut wires. The unit cell is shown on the right. The size of the unit cell is $0.789 \times 3.31 \times 4.26$ mm. The size of the SRR is 3×3 mm with azimuthal gap 0.157 mm. The wire width is 0.979 mm with a cut of 0.157 mm. Dashed line on the top panel shows the transmission for an array of wires. For the DNM, we found three transmission peaks. Note that the first transmission peak is right-handed. The two other peaks are left-handed, as is proved by the sign of n'_{eff} in the bottom panel.

7. Conclusion

The transfer matrix method has been proved to be very useful in the numerical investigation of double negative metamaterials. Although it can not compete with the commercial software, when the exact parameters of the DNM are required for the technological purposes, it provides us with a very good qualitative description of the investigated structures. As was shown in this paper (see also [6, 7, 8]), the TMM enables us to treat various shapes of the DNM and predict qualitatively their transport properties.

The transmission and the reflection are obtained in a straightforward way. The TMM data can be therefore directly used for the calculation of the effective parameters of the system.

An important property of the TMM is its ability to calculate the transmission for both polarizations. We have shown that some part of the EM wave changes its polarization when passes through the double negative medium. Thus, in experiments with a $\vec{E}||y$ wave as input we observe that some small part of the outgoing $\vec{E}||y$ wave does not experienced the left-handedness, because it propagates through the sample as a $\vec{E}||x$ wave. Outside the pass band, this “false wave” represents the only output, if the sample is big enough to absorb the “true wave” completely.

Due to the numerical analysis of results obtained by the TMM, there is no doubt today that the permittivity and permeability is negative in the resonance frequency interval. In the pass band, we calculated all electromagnetic parameters of the double negative medium. Further generalization of the present procedure is required, which incorporate also the change of the polarization of the EM wave as passes through the double negative system. This will be important for the analysis of the more complicated DNM structures.

We have shown that the double negative metamaterials are in fact triple negative materials. Thanks to the high transmission of the system, the imaginary part of the permittivity is negative, too. This surprising result seems to contradict our physical intuition. Nevertheless, it is not in contradiction with any basic physical law. To understand the sign of the effective parameters better, we also studied an another system -

periodic array of thin broken metallic wire - in which we found the imaginary part of the effective permeability to be negative [25]. Thus we believe that systems with negative sign of imaginary part of either *effective* permittivity or *effective* permeability might be quite often created in today's laboratories, although it may not be present in nature.

Our results show that the theoretical understanding of the electromagnetic properties of the DNM requires to extend the treatment of the propagation of EM waves in media which have both ϵ and μ negative and complex. This was never done in the standard EM textbooks. General formulas for the energy of the EM field [26] and for the transmission losses, applicable also for systems with complex permittivity and permeability are highly desired.

Acknowledgments

We want to thank D.R. Smith, for fruitful discussions. This work was supported by Ames Laboratory (contract. n. W-7405-Eng-82). Financial support of DARPA, NATO (Grant No. PST.CLG.978088) and APVT (Project n. APVT-51-021602) and EU project DALHM are also acknowledged.